JGR Biogeosciences

RESEARCH ARTICLE
10.1029/2019JG005498

A Non-steady State Model Based on Dual Nitrogen and Oxygen Isotopes to Constrain Moss Nitrate Uptake and Reduction

Xue-Yan Liu[1,2,3], Di Wu[1], Xin Song[4], Yu-Ping Dong[1], Chong-Juan Chen[1], Wei Song[1], Cong-Qiang Liu[1,2], and Keisuke Koba[3,5]

[1]Institute of Surface-Earth System Science, School of Earth System Science, Tianjin University, Tianjin, China, [2]State Key Laboratory of Environmental Geochemistry, Institute of Geochemistry, Chinese Academy of Sciences, Guiyang, China, [3]Institute of Agriculture, Tokyo University of Agriculture and Technology, Fuchu, Japan, [4]College of Life Sciences and Oceanography, Shenzhen University, Shenzhen, China, [5]Center for Ecological Research, Kyoto University, Kyoto, Japan

Key Points:
- A non-steady state isotope mass-balance model was used to evaluate moss nitrate sources and reduction
- Epilithic mosses acquire about half of their nitrate from the underlying soil substrates
- Nitrate contributed a low fraction of the total N in the studied mosses

Supporting Information:
- Supporting Information S1

Correspondence to:
X.-Y. Liu,
liuxueyan@tju.edu.cn

Citation:
Liu, X.-Y., Wu, D., Song, X., Dong, Y.-P., Chen, C.-J., Song, W., et al. (2020). A non-steady state model based on dual nitrogen and oxygen isotopes to constrain moss nitrate uptake and reduction. *Journal of Geophysical Research: Biogeosciences*, *125*, e2019JG005498. https://doi.org/10.1029/2019JG005498

Received 1 OCT 2019
Accepted 17 MAR 2020
Accepted article online 19 MAR 2020

Author Contributions:
Conceptualization: Xue-Yan Liu
Data curation: Xue-Yan Liu, Di Wu
Writing – review & editing: Xue-Yan Liu, Di Wu, Xin Song, Yu-Ping Dong

Abstract Epilithic mosses are early colonizers of the terrestrial biosphere, which constitute a special ecosystem regulating rock-atmosphere interactions. Terrestrial mosses can take up nitrate (NO_3^-), a major form of bioavailable N, from soil substrates. However, the importance of substrate NO_3^- relative to atmospheric NO_3^- remains unclear in moss NO_3^- utilization. This has prevented the understanding of moss NO_3^- dynamics and their responses to environmental N loadings. This study investigated monthly concentrations, $\delta^{15}N$, and $\delta^{18}O$ of NO_3^- in four epilithic moss species from August 2006 to August 2007 in Guiyang, southwestern China. We developed a non-steady state isotope mass-balance model to evaluate fractional contributions of atmospheric NO_3^- (Φ_{atm}) and soil NO_3^- (Φ_{soil}), moss NO_3^- uptake flux (F_{influx}), moss NO_3^- reduction flux ($F_{reduction}$), and the percentage of NO_3^- reduction in moss NO_3^- uptake ($f_{reduced}$). The monthly Φ_{soil} values averaged 53 ± 13% and the monthly $f_{reduced}$ values averaged 50 ± 35%. Both the monthly $F_{reduction}$ and $f_{reduced}$ increased as the monthly F_{influx} increased, particularly when the Φ_{soil} values were higher than Φ_{atm} values. However, the amount of annual NO_3^- reduction (219.7 ± 30.5 μg-N/g, dw) accounted for only 1.0 ± 0.2% of the bulk N of the mosses. We conclude that half of the NO_3^- in epilithic mosses is derived from the soil NO_3^- and that NO_3^- uptake from the soil induces moss NO_3^- reduction, but the total NO_3^- assimilation contributed a low fraction of the total N in the studied mosses. These findings are important for understanding N sources and N dynamics in terrestrial mosses.

1. Introduction

Since the industrial revolution, anthropogenic nitrogen (N) oxide emissions, atmospheric NO_3^- deposition, and soil NO_3^- availability have increased in many terrestrial environments (Galloway et al., 2008). Among terrestrial biota, mosses are believed to be sensitive and reliable indicators of atmospheric N loadings (Bragazza et al., 2005; Zechmeister et al., 2008). The major assumptions involved in this hypothesis include the following: (1) Most moss taxa lack stomata (at least in the gametophyte stage), with leaves only one cell thick and no cuticular barrier; (2) mosses lack efficient rooting and transport systems to take up nutrients from their growing substrates (Glime, 2007; Raven et al., 1998). Recently, moss-tissue NO_3^- was measured to determine atmospheric NO_3^- pollution or its deposition levels (Liu, Koba, Liu et al., 2012; Liu, Koba, Takebayashi, et al., 2012), but they also assumed that mosses derive NO_3^- completely or mainly from atmospheric deposition.

Despite their lack of roots, some moss species (either endohydric taxa, which move water within the plant through the internal conduction, or ectohydric taxa, which move and gain their water along the leafy surfaces) can actually transport nutrients upward (Aerts, 1996; Aldous, 2002; Glime, 2007). This can be accomplished through their leptoids (phloem-like cells) and hydroids (xylem-like cells) (e.g., *Polytrichum commune*; Reinhart & Thomas, 1981), or through capillary action (e.g., *Racomitrium lanuginosum*; Jónsdóttir et al., 1995) and plasmodesmata (Wells & Brown, 1996). Thus, terrestrial mosses can absorb the N in soil substrates (Ayres et al., 2006; Wang et al., 2014). In a lowland tropical rainforest in Costa Rica, the bulk $\delta^{15}N$ in epiphytic mosses suggests that N is taken up from the canopy soils (dead organic matter

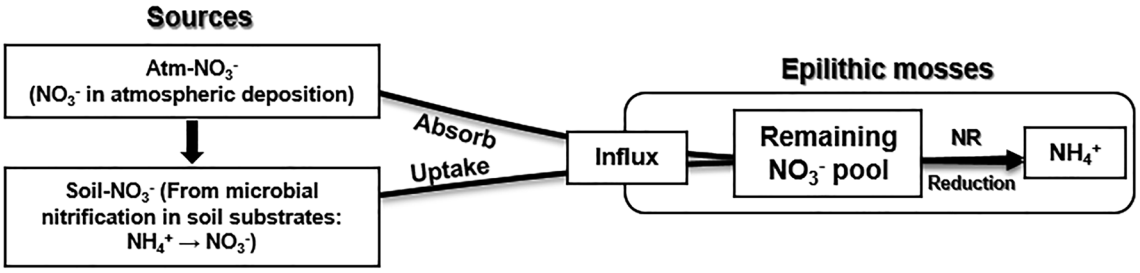

Figure 1. Simplified scheme of the influx and reduction of atmospheric-derived NO_3^- (atm-NO_3^-) and soil-derived NO_3^- (soil-NO_3^-) in epilithic mosses. NR: nitrate reductase. The efflux of NO_3^- out of the moss tissues is assumed to be negligible.

accumulated in branch crotches, on branches, and on boles; Wania et al., 2002). In alpine sites in Scotland and China, ^{15}N tracers added to soils were recovered in terricolous mosses although the proportions were relatively low (2–9% in Ayres et al., 2006; 17–30% in Wang et al., 2014). Nitrate is highly mobile and soil-NO_3^- may enter the moss cells by diffusion, potentially through cotransport with positively charged ions (Raven et al., 1998). However, quantifying the in situ contributions of NO_3^- derived from nitrification in soil substrates (soil-NO_3^-) and NO_3^- from atmospheric deposition (atm-NO_3^-) to the total NO_3^- influx into mosses is difficult (Figure 1). Therefore, the degree of moss NO_3^- acquisition from soil substrates has not been adequately quantified, so the impact of soil-NO_3^- on moss NO_3^- uptake and metabolism is unknown. Importantly, NO_3^- uptake into mosses from the soil must be quantified to accurately determine the budget of NO_3^- influx into mosses and to understand how the sizes of NO_3^- pools in mosses respond to atmospheric NO_3^- pollution.

Enzymatic NO_3^- reduction by nitrate reductase (NR) in the cytosol of plant-tissue cells and subsequent photosynthetic N assimilation (Bloom et al., 1992; Tcherkez & Hodges, 2008) is the other important process regulating the pool sizes of plant-tissue NO_3^-. The levels of nitrate reductase activity (NRA) (Stewart et al., 1993) have traditionally been considered to reflect potential NO_3^- reduction in plants (e.g., Atkin et al., 1993; Atkin & Cummins, 1994; Nadelhoffer et al., 1996). However, NRA is inducible by NO_3^-, so NRA may be overestimated by experimental NO_3^- additions during NRA assays (Tischner, 2000). Moreover, NRA assays may also be influenced by the addition of ethanol, pH adjustment, vacuum infiltration, or plant pigments during colorimetrical measurements of NO_3^- and NO_2^- concentrations (Liu et al., 2014). Therefore, the real rates of moss NO_3^- reduction, the responses of moss NO_3^- reduction to NO_3^- uptake, and the importance of NO_3^- assimilation to the bulk N in moss biomass remain uncertain.

Stable isotopes can elucidate plant N uptake, primary metabolic processes, and the responses of these two processes to changes in N availability (Craine et al., 2015; Hobbie & Högberg, 2012; Tcherkez & Hodges, 2008). Recently, the conversion of NO_3^- in plant extracts to N_2O by a denitrifier (Casciotti et al., 2002) was used to measure the concentrations and the natural N and O isotopes of NO_3^- in moss tissues, which provided new parameters for determining moss NO_3^- dynamics (Liu, Koba, Liu, et al., 2012; Liu, Koba, Takebayashi, et al., 2012; Liu, Koba, Yoh, et al., 2012; Liu et al., 2014, 2018). Compared with the NRA assay, the natural isotopic abundances of NO_3^- in plant tissues provide an improved estimate of in situ NO_3^- reduction in wild terrestrial plants (Bloom et al., 2014; Liu et al., 2014, 2018; Yoneyama & Tanaka, 1999). Because mosses have relatively simple tissue structures (Raven et al., 1998), the entry of the source NO_3^- into moss cells may not have substantial isotopic effects (verified in phytoplanktons; Granger et al., 2004, 2010). In addition, excess N supply promotes NO_3^- efflux from the roots (Evans et al., 1996; Mariotti et al., 1982). Due to the low N supply from substrates, such as rocks and woods to mosses, the NO_3^- efflux from moss tissues may be negligible. For these reasons, the N and O isotopes of moss NO_3^- can be used to differentiate between the fractional contributions of soil-NO_3^- and atm-NO_3^- to the moss NO_3^- influx (Figure 1). Due to enrichments in ^{15}N and ^{18}O during partial NO_3^- reduction by NR (Ledgard et al., 1985; Tcherkez & Farquhar, 2006), the isotopic values of the NO_3^- remaining in the mosses will be higher than those of the initial mixture of atm-NO_3^- and soil-NO_3^-. Isotopic discriminations of NR in mosses ($^{15}\Delta = 12.1‰$ and $^{18}\Delta = 14.4‰$ measured for *Hypnum plumaeforme*; Liu, Koba, Yoh, & Liu, 2012) are generally similar to those measured for enzymatic NO_3^- reduction in vascular plants (Ledgard

et al., 1985; Liu et al., 2014; Tcherkez & Farquhar, 2006). Accordingly, by considering the isotopic fractionation of NR in mosses, the proportional contributions of atm-NO_3^- and soil-NO_3^- to the total NO_3^- influx into mosses and the moss NO_3^--reduction dynamics can be evaluated by combining the isotopic signatures of the moss-tissue NO_3^- pool with the isotopic signatures of atm-NO_3^- and soil-NO_3^-.

Because moss NO_3^- concentrations and isotopes have only been studied at single time points, temporal variations in moss NO_3^- dynamics remain unclear (Liu et al., 2014). As a consequence, the interpretation of moss-tissue NO_3^- concentrations and isotopes for source contributions and enzymatic reduction has only been qualitative. Moreover, the steady-state assumption commonly adopted in these previous studies (Liu, Koba, Liu, et al., 2012; Liu, Koba, Takebayashi, et al., 2012; Liu, Koba, Yoh, & Liu, 2012) may over simplify the real world in which both the concentration and isotope compositions of moss NO_3^- are likely to change over time. The lack of a dynamic method for correctly quantifying the atm-NO_3^- and soil-NO_3^- contributions as well the NO_3^- influx and reduction in the open system of moss-tissue NO_3^- has limited our understanding of moss NO_3^- assimilation and its responses to atmospheric NO_3^- loading.

In this context, we investigated the NO_3^- concentrations and isotopic values of four epilithic moss species from an urban site in China for which the isotopic compositions of the atm-NO_3^- and soil-NO_3^- sources have been previously characterized and the moss NO_3^- reduction has been inferred to be substantially inhibited by the reduced N supply that is higher than the NO_3^- supply (Liu et al., 2017; Liu, Koba, Takebayashi, et al., 2012). We used a non-steady-state isotope mass-balance model to calculate the fractional contributions of atm-NO_3^- and soil-NO_3^- to the moss NO_3^- uptake, the moss NO_3^- influx, the moss NO_3^- reduction flux, and the percentage of reduced NO_3^- in the total NO_3^- uptake of the mosses. This allowed us to assess the importance of soil-NO_3^- relative to atm-NO_3^- in regulating moss NO_3^- uptake and the importance of NO_3^- reduction in moss bulk N assimilation.

2. Materials and Methods

2.1. Study Site

This study was conducted at Mt. Guanfeng in the southeast part of downtown Guiyang (26°34.5′N, 106°43.3′E). Guiyang is the capital city of Guizhou Province, and it is also one of the major cities in southwestern China suffering from severe acid deposition since the 1980s (Liu et al., 2017). The inorganic N deposition is dominated by NH_4^+-N (71%), and fossil and nonfossil NO_x have comparable contributions to local NO_3^- deposition in urban environments (Liu et al., 2017). It has a typical subtropical monsoon climate, and most of the landforms are at altitudes of 1,000–1,500 m. The mean annual relative humidity is 86%. During the study period from August 2006 to August 2007, the mean annual temperature was 16.2°C and the total rainfall was 984 mm (Figure S1 in the supporting information). Rainfall in this region is distinctly seasonal, with about 60% falling in the warmer plant-growing months from April to September (Figure S1).

2.2. Sample Collection and Analyses

Four epilithic moss species (*Bryum argenteum* Hedw., *Eurohypnum leptothallum* (C. Muell.) Ando, *Haplocladium microphyllum* (Hedw.) Broth, and *Hypnum plumaeforme* Wils.) were selected because they were more available than other species. They are also widespread moss species, and *E. leptothallum* and *H. microphyllum* have previously been used to evaluate environmental pollution and deposition (Liu et al., 2007). *H. plumaeforme* and *B. argenteum* may have a significant tolerance for pollution based on their abilities to colonize diverse habitats in disturbed areas.

The mosses were sampled at the end of each month (24th–31st) from August 2006 until August 2007 (see details in Dong et al., 2017). The sampling sites were located on the upper part of the mountain (1065 ± 10 m) in an attempt to avoid sunlight differences and the influence of surface-water splashing. The moss clusters on rocks had thin organic soil layers (about 3–5 mm thick) at the study site. Green moss tissues (including mature and growing shoots, about 2–4 cm in thickness) were collected each time from a large lump of epilithic mosses (about 50–200 cm^2 in areas, in the presence of at least one of the studied moss species). Each month, three to six subsampling sites with clumps or mats of moss were sampled (about 3–5 cm^2 of moss layers were scraped down at each site during each collection), separated by species, and mixed as a composite sample of each species (totally $n = 13$ for each species). There were no clear dead tissue layers

lower in the moss cushion, and thus, the moss samples can be considered as whole that directly attached to the substrate and received and retained atmospheric deposition evenly.

Moss NO_3^- extraction and the analyses of the concentrations and isotopic values were conducted following the same procedure used in our earlier studies (see Liu, Koba, Liu, et al., 2012; Liu, Koba, Takebayashi, et al., 2012; Liu et al., 2018, for details). Briefly, the NO_3^- in the dried and ground moss samples was extracted using deionized water. An NO_3^--free media with a denitrifier (*Pseudomonas aureofaciens*) (ATCC# 13985) was used to convert the moss-tissue NO_3^- to N_2O. Then, the concentrations and amount of N_2O were measured using a gas chromatograph equipped with an electron capture detector (GC/ECD, GC-14B; Shimadzu Corp., Kyoto, Japan), and the results were used to calculate the NO_3^- concentrations of the mosses. After this, all of the N_2O in the sample vial was purified, cryogenically focused, and introduced into an isotope-ratio mass spectrometer (Delta XP; Thermo Fisher Scientific Inc., Yokohama, Japan) coupled with a Precon (ThermoFinnigan) and a GC (Agilent, HP6890, Hewlett Packard Co., Palo Alto, CA, USA) equipped with a Poraplot column (25 m × 0.32 mm), and a GC interface III (Thermo Fisher Scientific Inc., Yokohama, Japan), which were used for the N and O isotopic measurements. The denitrifier (*P. aureofaciens*) causes relatively little incorporation of O atoms from the water into the N_2O (Casciotti et al., 2002). The calibration curve between the measured isotope ratios of N_2O and those of NO_3^- was conducted using isotopic reference materials (IAEA-NO_3, USGS 32, USGS 34, and USGS 35). The measured $^{18}O/^{16}O$ ratios of samples have been corrected for both the O isotopic fractionation during the conversion of NO_3^- to N_2O and the O exchange between the water and N_2O product (Casciotti et al., 2002). The analytical precision was better than 0.2‰ for $\delta^{15}N$-NO_3^- and 0.5‰ for $\delta^{18}O$-NO_3^-. The natural abundances of ^{15}N ($\delta^{15}N$) and ^{18}O ($\delta^{18}O$) are expressed in parts per mil (‰).

$$\delta^{15}\mathrm{N} \text{ or } \delta^{18}\mathrm{O} = \left(R_{\mathrm{sample}}/R_{\mathrm{standard}} - 1\right),$$

where $R = {}^{15}N/{}^{14}N$ or $^{18}O/^{16}O$ in the samples and standards (atmospheric N_2 and VSMOW, respectively).

2.3. Theoretical Basis of the Non-steady State Isotope Mass-Balance Model

The O isotope exchange between NO_3^- and water are measurable only at 50–80°C and pH = 0.6–1.1, but they are exceedingly slow under natural conditions (25°C and pH = 7, with an estimated half-life for isotope exchange of 5.5×10^9 years (Kaneko & Poulson, 2013). Terrestrial mosses, even under high ammonium supply, have tissue pH values of greater than 4.0 (Paulissen et al., 2004). In addition, the denitrifier (*P. aureofaciens*) can reduce both the NO_3^- and nitrite (NO_2^-) in the extracts of the moss samples to N_2O. However, because of the generally high ratios (5–20) of nitrite reductase activities (NiRA) to NRA (Beevers & Hageman, 1980; Ledgard et al., 1985), NO_2^- is quickly converted to ammonium and is often quite negligible relative to the NO_3^- pool in sunlit plants. Therefore, the $\delta^{18}O$ values measured for the NO_3^- in the mosses can be used to elucidate the uptake of external NO_3^- sources and NO_3^- reduction in mosses.

Our sampling strategy, which was described in the above section and results were shown in Figure 2, allowed us to calculate Φ_{atm}, Φ_{soil}, F_{influx}, $F_{\mathrm{reduction}}$, and f_{reduced} values (defined in Table 1) using a non-steady state isotope mass-balance approach. Below, we explain the relevant assumptions, theory, and equations that form the basis of this modeling approach based on the dual N and O isotopes in NO_3^-.

First, assuming no substantial isotopic effect during the absorption of NO_3^- into the mosses (Craine et al., 2015; Granger et al., 2004, 2010; Robinson et al., 1998; Tcherkez & Hodges, 2008; Werner & Schmidt, 2002), we have the following equations (1 and 2).

$$\delta^{15}\mathrm{N}_{\mathrm{influx}} = \Phi_{\mathrm{atm}} \times \delta^{15}\mathrm{N}_{\mathrm{atm}} + \Phi_{\mathrm{soil}} \times \delta^{15}\mathrm{N}_{\mathrm{soil}}, \text{ where } \Phi_{\mathrm{atm}} + \Phi_{\mathrm{soil}} = 1, \quad (1)$$

$$\delta^{18}\mathrm{O}_{\mathrm{influx}} = \Phi_{\mathrm{atm}} \times \delta^{18}\mathrm{O}_{\mathrm{atm}} + \Phi_{\mathrm{soil}} \times \delta^{18}\mathrm{O}_{\mathrm{soil}}, \text{ where } \Phi_{\mathrm{atm}} + \Phi_{\mathrm{soil}} = 1, \quad (2)$$

where the $\delta^{15}N_{atm}$ and $\delta^{18}O_{atm}$ values were previously measured for the NO_3^- in precipitation collected at the study site on Mt. Guanfeng in 2008–2009 (the sampling and analysis of these values (Figure 3) are described in Liu et al., 2017), which were separated into cooler and warmer months during the calculations in the present study. The $\delta^{15}N_{soil}$ and $\delta^{18}O_{soil}$ values were also previously measured for epilithic mosses on Mt. Guanfeng in July 2010 (the sampling and analysis of these values (Figure 3) are

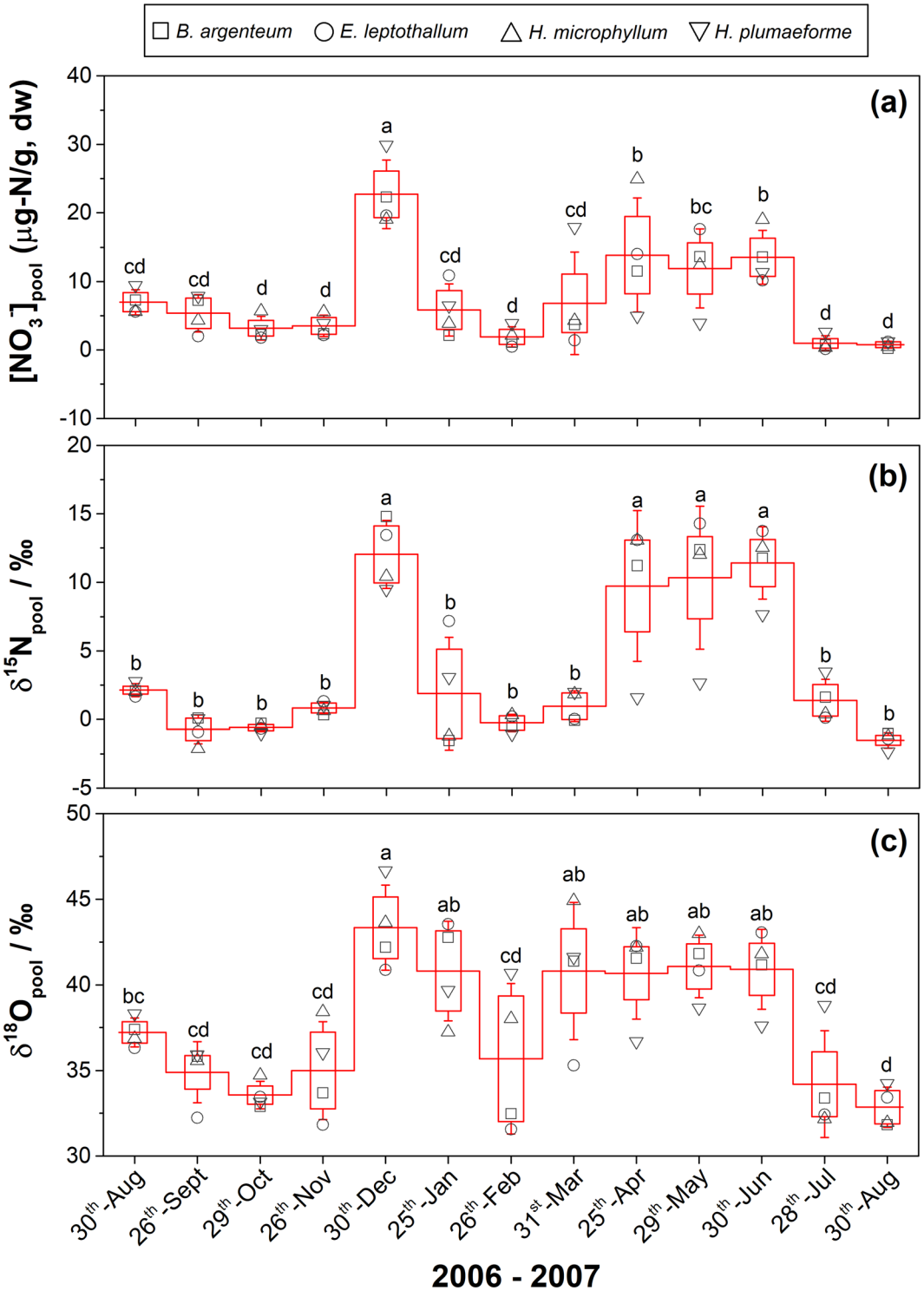

Figure 2. (a) Concentrations ($[NO_3^-]_{pool}$), (b) $\delta^{15}N$ values ($\delta^{15}N_{pool}$), and (c) $\delta^{18}O$ values ($\delta^{18}O_{pool}$) of NO_3^- in epilithic mosses collected monthly from August 2006 to August 2007 in Guiyang, SW China. The box encompasses the 25th–75th percentiles, the whiskers and red H lines across the boxes show the SD and mean values, respectively. The different letters above the boxes mark significant differences at the $p < 0.05$ level.

Table 1
Symbols Used in the Equations in This Paper

Symbol	Meaning
$\delta^{15}N_{atm}$	$\delta^{15}N$ values of NO_3^- in atmospheric deposition (‰)
$\delta^{18}O_{atm}$	$\delta^{18}O$ values of NO_3^- in atmospheric deposition (‰)
$\delta^{15}N_{soil}$	$\delta^{15}N$ values of NO_3^- in underlying soil substrates of mosses (‰)
$\delta^{18}O_{soil}$	$\delta^{18}O$ values of NO_3^- in underlying soil substrates of mosses (‰)
Φ_{atm}	Fractional contribution of atmospheric NO_3^- to NO_3^- in mosses (%)
Φ_{soil}	Fractional contribution of soil NO_3^- to NO_3^- in mosses (%)
$\delta^{15}N_{influx}$	$\delta^{15}N$ values of NO_3^- influx into mosses (‰)
$\delta^{18}O_{influx}$	$\delta^{18}O$ values of NO_3^- influx into mosses (‰)
$[NO_3^-]_{pool}$	Concentrations of remaining NO_3^- pool in mosses (μg-N/g, dw) (Figure 2a)
$\delta^{15}N_{pool}$	$\delta^{15}N$ values of remaining NO_3^- pool in mosses of each collection (‰) (Figure 2b)
$\delta^{18}O_{pool}$	$\delta^{18}O$ values of remaining NO_3^- pool in mosses of each collection (‰) (Figure 2c)
$\delta^{15}N_{reduction}$	$\delta^{15}N$ values of NO_3^- that has been reduced by NR in mosses during a given time step (‰)
$\delta^{18}O_{reduction}$	$\delta^{18}O$ values of NO_3^- that has been reduced by NR in mosses during a given time step (‰)
$^{15}\Delta$	^{15}N discrimination of the NR reaction in mosses (‰)
$^{18}\Delta$	^{18}O discrimination of the NR reaction in mosses (‰)
F_{influx}	The influx of moss NO_3^- uptake, which represents the total amount of moss NO_3^- absorption during a given time step (μg-N/g, dw)
$F_{reduction}$	Flux of NO_3^- reduction in mosses, which represents the amount of moss NO_3^- reduction during a given time step (μg-N/g, dw)
$f_{reduced}$	Fractions of NO_3^- that has been reduced in the total of remaining and newly-absorbed NO_3^- in mosses during a given time step (%)

described in Liu et al., 2013). The $\delta^{15}N_{atm}$ values were often similar to the $\delta^{15}N_{soil}$ values, but the $\delta^{18}O_{atm}$ values were distinctly higher than the $\delta^{18}O_{soil}$ values (Kendall et al., 2007; Liu et al., 2018; Michalski et al., 2004). Despite this, the isotopic values of the soil-NO_3^- at our study site were only previously measured once, so the source isotope variabilities between the years and locations may influence the calculations in this study.

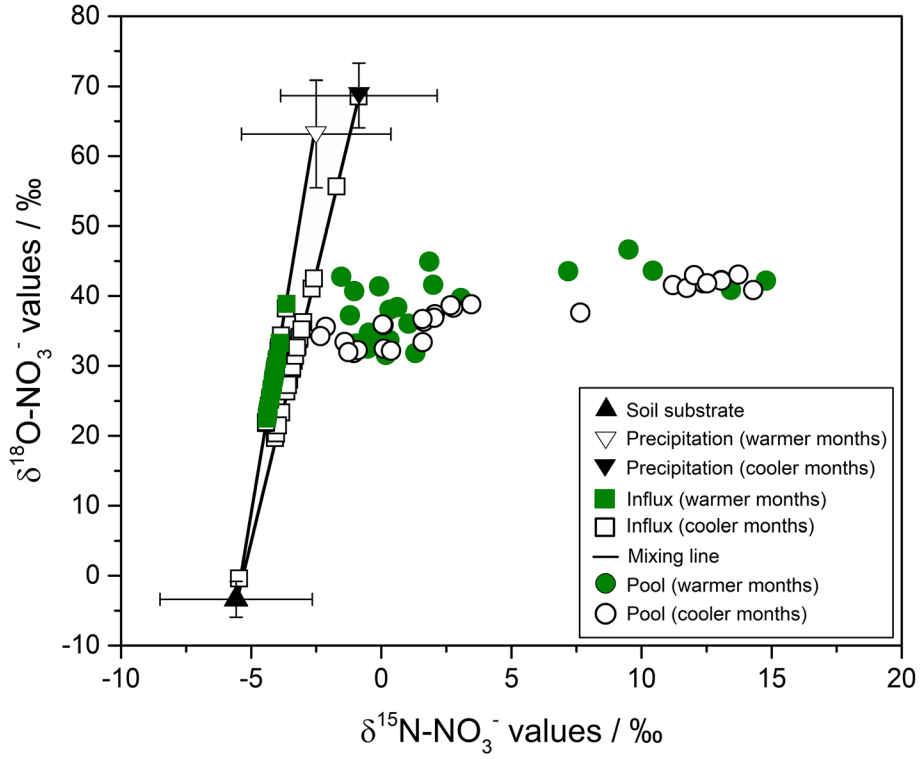

Figure 3. Distributions of $\delta^{15}N$ and $\delta^{18}O$ for NO_3^- in precipitation (n = 17 and 27 for cooler and warmer months, respectively; Liu et al., 2017), soil substrates (n = 3; Liu, Koba, Makabe, & Liu, 2013), NO_3^- influx into mosses, and the remaining NO_3^- pool in the tissues of the epilithic mosses from Mt. Guanfeng in Guiyang, SW China. The $\delta^{15}N$ and $\delta^{18}O$ values of the NO_3^- influx into the mosses were calculated using the corresponding Φ_{atm} and Φ_{soil} values (Figure 4a).

Because of the distinct variabilities in both the $[NO_3^-]_{pool}$ and the isotopic values among the moss samples collected throughout the year (Figure 2), we considered the moss-tissue NO_3^- dynamics to be an open non-steady state isotopic system. Assuming no substantial efflux of NO_3^- from the moss tissues (explained in the section 1), we have equations 3–5.

$$\Delta[NO_3^-]_{pool} = F_{\text{influx}} - F_{\text{reduction}}, \tag{3}$$

$$^{15}\Delta = \delta^{15}N_{\text{pool}} - \delta^{15}N_{\text{reduction}}, \tag{4}$$

$$^{18}\Delta = \delta^{18}O_{\text{pool}} - \delta^{18}O_{\text{reduction}}, \tag{5}$$

where the $\Delta[NO_3^-]_{\text{pool}}$ values are calculated as $[NO_3^-]_{\text{pool(t)}} - [NO_3^-]_{\text{pool}(t-1)}$ (t = 1, 2, ..., 13, corresponding to September of 2006, October of 2006, ..., August of 2007, Figure 2a), and the $^{15}\Delta$ and $^{18}\Delta$ values are 12.1‰ and 14.4‰ for the mosses, respectively (Liu, Koba, Yoh, & Liu, 2012). Based on equation 3, we have equation 6 for N isotopes and equation 7 for O isotopes.

$$\Delta\left([NO_3^-]_{\text{pool}} \times \delta^{15}N_{\text{pool}}\right) = F_{\text{influx}} \times \delta^{15}N_{\text{influx}} - F_{\text{reduction}} \times \delta^{15}N_{\text{reduction}}, \tag{6}$$

$$\Delta\left([NO_3^-]_{\text{pool}} \times \delta^{18}O_{\text{pool}}\right) = F_{\text{influx}} \times \delta^{18}O_{\text{influx}} - F_{\text{reduction}} \times \delta^{18}O_{\text{reduction}}. \tag{7}$$

Because $\Delta([NO_3^-]_{\text{pool}} \times \delta^{15}N_{\text{pool}}) = \delta^{15}N_{\text{pool}} \times \Delta[NO_3^-]_{\text{pool}} + [NO_3^-]_{\text{pool}} \times \Delta\delta^{15}N_{\text{pool}} + \Delta[NO_3^-]_{\text{pool}} \times \Delta\delta^{15}N_{\text{pool}}$, equation 6 can be rearranged to obtain equation 8.

$$\begin{aligned}&\delta^{15}N_{\text{pool}} \times \Delta[NO_3^-]_{\text{pool}} + [NO_3^-]_{\text{pool}} \times \Delta\delta^{15}N_{\text{pool}} + \Delta[NO_3^-]_{\text{pool}} \times \Delta\delta^{15}N_{\text{pool}} \\ &= F_{\text{influx}} \times \delta^{15}N_{\text{influx}} - F_{\text{reduction}} \times \delta^{15}N_{\text{reduction}}.\end{aligned} \tag{8}$$

Because $\Delta([NO_3^-]_{\text{pool}} \times \delta^{18}O_{\text{pool}}) = \delta^{18}O_{\text{pool}} \times \Delta[NO_3^-]_{\text{pool}} + [NO_3^-]_{\text{pool}} \times \Delta\delta^{18}O_{\text{pool}} + \Delta[NO_3^-]_{\text{pool}} \times \Delta\delta^{18}O_{\text{pool}}$, equation 7 can be rearranged to obtain equation 9.

$$\begin{aligned}&\delta^{18}O_{\text{pool}} \times \Delta[NO_3^-]_{\text{pool}} + [NO_3^-]_{\text{pool}} \times \Delta\delta^{18}O_{\text{pool}} + \Delta[NO_3^-]_{\text{pool}} \times \Delta\delta^{18}O_{\text{pool}} \\ &= F_{\text{influx}} \times \delta^{18}O_{\text{influx}} - F_{\text{reduction}} \times \delta^{18}O_{\text{reduction}},\end{aligned} \tag{9}$$

where the $\Delta\delta^{15}N_{\text{pool}}$ and $\Delta\delta^{18}O_{\text{pool}}$ values are calculated as $\Delta\delta^{15}N_{\text{pool(t)}} - \Delta\delta^{15}N_{\text{pool}(t-1)}$ and $\Delta\delta^{18}O_{\text{pool(t)}} - \Delta\delta^{18}O_{\text{pool}(t-1)}$, respectively ($t$ = 1, 2, ..., 13, corresponding to September of 2006, October of 2006, ..., August of 2007; Figures 2b and 2c).

By combining equation 3 with equation 4, equation 8 can be rearranged to obtain equation 10 after removing $(\delta^{15}N_{\text{pool}} \times \Delta[NO_3^-]_{\text{pool}})$ and combining similar terms.

$$[NO_3^-]_{\text{pool}} \times \Delta\delta^{15}N_{\text{pool}} + \Delta[NO_3^-]_{\text{pool}} \times \Delta\delta^{15}N_{\text{pool}} = F_{\text{influx}} \times \left(\delta^{15}N_{\text{influx}} - \delta^{15}N_{\text{pool}} + {}^{15}\Delta\right) - \Delta[NO_3^-]_{\text{pool}} \times {}^{15}\Delta. \tag{10}$$

By combining equation 3 with equation 5, equation 9 can be rearranged to obtain equation 11 by removing $(\delta^{18}O_{\text{pool}} \times \Delta[NO_3^-]_{\text{pool}})$ and combining similar terms.

$$[NO_3^-]_{\text{pool}} \times \Delta\delta^{18}O_{\text{pool}} + \Delta[NO_3^-]_{\text{pool}} \times \Delta\delta^{18}O_{\text{pool}} = F_{\text{influx}} \times \left(\delta^{18}O_{\text{influx}} - \delta^{18}O_{\text{pool}} + {}^{18}\Delta\right) - \Delta[NO_3^-]_{\text{pool}} \times {}^{18}\Delta. \tag{11}$$

Then, after combining equation 10 with equation 1, we can rearrange it to obtain equation 12.

$$\begin{aligned}&[NO_3^-]_{\text{pool}} \times \Delta\delta^{15}N_{\text{pool}} + \Delta[NO_3^-]_{\text{pool}} \times \Delta\delta^{15}N_{\text{pool}} = F_{\text{influx}} \times \left(\Phi_{\text{atm}} \times \delta^{15}N_{\text{atm}} + (1-\Phi_{\text{atm}}) \times \delta^{15}N_{\text{soil}}\right) \\ &-F_{\text{influx}} \times \delta^{15}N_{\text{pool}} + F_{\text{influx}} \times {}^{15}\Delta - \Delta[NO_3^-]_{\text{pool}} \times {}^{15}\Delta.\end{aligned} \tag{12}$$

After combining equation 11 with equation 2, we can rearrange it to obtain equation 13.

$$[NO_3^-]_{pool} \times \Delta\delta^{18}O_{pool} + \Delta[NO_3^-]_{pool} \times \Delta\delta^{18}O_{pool} = F_{influx} \times \left(\Phi_{atm} \times \delta^{18}O_{atm} + (1-\Phi_{atm}) \times \delta^{18}O_{soil}\right) \quad (13)$$
$$-F_{influx} \times \delta^{18}O_{pool} + F_{influx} \times {}^{18}\Delta - \Delta[NO_3^-]_{pool} \times {}^{18}\Delta.$$

According to equation 12, we get equation 14 for calculating the F_{influx} values.

$$F_{influx} = \left([NO_3^-]_{pool} \times \Delta\delta^{15}N_{pool} + \Delta[NO_3^-]_{pool} \times \Delta\delta^{15}N_{pool} + \Delta[NO_3^-]_{pool} \times {}^{15}\Delta\right) / \quad (14)$$
$$\left(\Phi_{atm} \times \delta^{15}N_{atm} + (1-\Phi_{atm}) \times \delta^{15}N_{soil} - \delta^{15}N_{pool} + {}^{15}\Delta\right).$$

By combining equation 13 with equation 14, we get equation 15 for calculating the Φ_{atm} values.

$$\Phi_{atm} = \left\{\left(\delta^{18}O_{soil} + {}^{18}\Delta - \delta^{18}O_{pool}\right) \times \left(\Delta\delta^{15}N_{pool} \times \left([NO_3^-]_{pool} + \Delta[NO_3^-]_{pool}\right) + \Delta[NO_3^-]_{pool} \times {}^{15}\Delta\right)\right. \quad (15)$$
$$- \left(\delta^{15}N_{soil} + {}^{15}\Delta - \delta^{15}N_{pool}\right) \times \left(\Delta\delta^{18}O_{pool} \times \left([NO_3^-]_{pool} + \Delta[NO_3^-]_{pool}\right) + \Delta[NO_3^-]_{pool} \times {}^{18}\Delta\right)\Big\} /$$
$$\left\{\left(\Delta\delta^{18}O_{pool} \times \left([NO_3^-]_{pool} + \Delta[NO_3^-]_{pool}\right) + \Delta[NO_3^-]_{pool} \times {}^{18}\Delta\right) \times \left(\delta^{15}N_{atm} - \delta^{15}N_{soil}\right)\right.$$
$$\left. + \left(\Delta\delta^{15}N_{pool} \times \left([NO_3^-]_{pool} + \Delta[NO_3^-]_{pool}\right) + \Delta[NO_3^-]_{pool} \times {}^{15}\Delta\right) \times \left(\delta^{18}O_{soil} - \delta^{18}O_{atm}\right)\right\}$$

Using the Φ_{atm} values 15, the Φ_{soil} values ($\Phi_{soil} = 1 - \Phi_{atm}$, rearranged from equation 1) and F_{influx} values 14 can be calculated. Then, the $F_{reduction}$ values can be calculated using the F_{influx} values 14 and equation 3 (rearranged as $F_{reduction} = F_{influx} - \Delta[NO_3^-]_{pool}$).

During the calculation, the first sampling on 30 August 2006 was used as the initial value for the first time step, and then, we solved for the Φ_{atm}, Φ_{soil}, F_{influx}, and $F_{reduction}$ values for the 12 time steps from September of 2006 to August of 2007 (Figure 4). Finally, the fractions of NO_3^- that were reduced during a given time step ($F_{reduction(t)}$) in the sum of the initial NO_3^- (i.e., the measured $[NO_3^-]_{pool(t-1)}$) and the newly absorbed NO_3^- during that time step ($F_{influx(t)}$) ($f_{reduced(t)}$, defined in Table 1) were estimated for 12 time steps from September of 2006 to August of 2007 using equation 16 (Figure 4).

$$f_{reduced(t)} = F_{reduction(t)} / \left([NO_3^-]_{pool(t-1)} + F_{influx(t)}\right). \quad (16)$$

The uncertainties in the calculated Φ_{atm}, Φ_{soil}, F_{influx}, $F_{reduction}$, and $f_{reduced}$ values of each collection of each moss species were estimated as propagated errors obtained using a Monte Carlo method (MCM). Briefly, we ran 300 trials for the MCM in the software of Microsoft Excel-Add-In and calibrated the standard deviations (SD values) of the known parameters to match the corresponding true values. The true SD values were 2.9‰ (warmer months) and 3.0‰ (cooler months) for $\delta^{15}N_{atm}$, 7.7‰ (warmer months) and 4.6‰ (cooler months) for $\delta^{18}O_{atm}$, 0.0‰ for $\delta^{15}N_{soil}$, and 2.5‰ for $\delta^{18}O_{soil}$ (Figure 3). The propagated errors of the calculated parameters are expressed as the SD value of 300 trials. The propagated SD values for each sampling of each moss species are shown in Figure 4 and averaged 2.3% (0.0–6.9%) for Φ_{atm} and Φ_{soil}, 0.6 μg-N/g, dw (0.0–6.2 μg-N/g, dw) for F_{influx} and $F_{reduction}$, and 0.5% (0.0–4.6%) for $f_{reduced}$ (Figure 4).

2.4. Statistics

All of the analyses were conducted using the SPSS 12.0 software package for Windows (SPSS Science, Chicago, USA). The Tukey honest significant difference (Tukey HSD) and the least significant difference (LSD) tests of the one-way analysis of variance (ANOVA) were used to identify significant differences in the moss NO_3^- parameters among the moss species and among collections. The variance components were analyzed to estimate the explanatory power and the relative importance of the moss species and samplings in the variations of each moss NO_3^- parameter (Figure S3). The single correlation analysis was used to examine the relationships between the moss F_{influx}, $F_{reduction}$, and $f_{reduced}$ values (Figure 5). The mean ± SD values were shown. Statistically significant differences were set at p values <0.05.

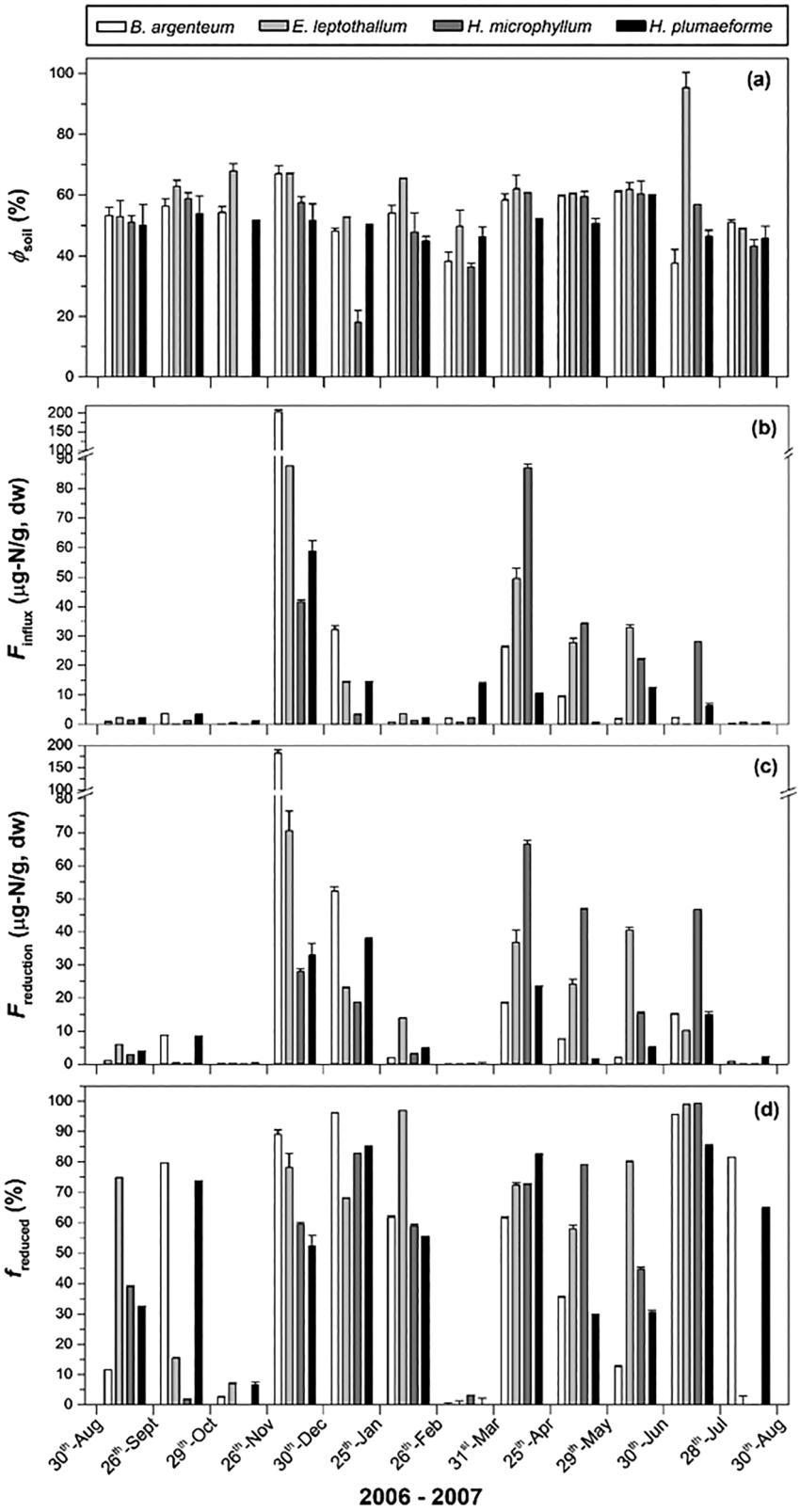

Figure 4. (a) Φ_{soil}, (b) F_{influx}, (c) $F_{reduction}$, and (d) $f_{reduced}$ values of the epilithic mosses collected monthly from August 2006 to August 2007 in Guiyang, SW China. The Φ_{soil}, F_{influx}, $F_{reduction}$, and $f_{reduced}$ values were calculated using equations 1, 3, and 14–16, and their uncertainties (shown as SD values; whiskers) were estimated using the Monte Carlo method.

3. Results

3.1. Moss NO_3^- Concentrations and Isotopes

The concentrations, $\delta^{15}N$, and $\delta^{18}O$ values of the NO_3^- in the studied mosses varied from 0.1 μg-N/g, dw to 29.9 μg-N/g, dw; −2.3‰ to 14.8‰; and 31.6‰ to 46.7‰, respectively (Figure 2). The $\delta^{15}N_{moss}$ values were higher than those of the atm-NO_3^- and soil-NO_3^- sources (Figure 3). The moss-tissue NO_3^- had much lower $\delta^{18}O$ than the precipitation NO_3^-, but the $\delta^{18}O_{moss}$ values were between the atm-NO_3^- and soil-NO_3^- $\delta^{18}O$ values (Figure 3). In general, neither the concentrations nor the isotopic values of the tissue NO_3^- differed significantly between the four moss species when considering all of the collections. The variance component analyses showed that the differences between the species contributed much less to the variations in the moss NO_3^- parameters than the sampling time did (Figure S3). Increased concentrations and isotopic values of the moss NO_3^- occurred in some months (particularly for April, May, June, and December) compared with the other nine collections (Figure 2).

3.2. Estimated Φ_{atm}, Φ_{soil}, F_{influx}, $F_{reduction}$, and $f_{reduced}$ Values

For all 12 time steps of the four moss species ($n = 48$), the mean ± SD values (data ranges) were 47 ± 13% (5–100%) for Φ_{atm} (calculated using equation 15), 53 ± 13% (0–96%) for Φ_{soil} 1, and 50 ± 35% (0–99%) for $f_{reduced}$ 16 (Figures 4a and 4d). The Φ_{atm}, Φ_{soil}, and $f_{reduced}$ values did not differ significantly when comparing all 12 collections. *B. argenteum* had higher F_{influx} and $F_{reduction}$ values (calculated by equations 14 and 3), and *H. plumaeforme* had lower values than the other moss species (Figures 4b and 4c). On a dry weight basis, the total annual F_{influx} values of the 12 collections were 282.9 μg-N/g for *B. argenteum*, 220.2 μg-N/g for *E. leptothallum*, 222.9 μg-N/g for *H. microphyllum*, and 126.8 μg-N/g/yr for *H. plumaeforme*. Similarly, the total $F_{reduction}$ values of 12 collections were 290.4 μg-N/g for *B. argenteum*, 225.2 μg-N/g for *E. leptothallum*, 227.9 μg-N/g for *H. microphyllum*, and 135.3 μg-N/g for *H. plumaeforme*. Across the four moss species, the total annual F_{influx} and $F_{reduction}$ values averaged 213.2 ± 34.5 and 219.7 ± 30.5 μg-N/g, respectively.

The variance component analyses shows that the species contributed much less to the variations in the Φ_{soil}, F_{influx}, $F_{reduction}$, and $f_{reduced}$ values than the sampling time did (Figure S3). The resolved monthly Φ_{atm}, Φ_{soil}, F_{influx}, $F_{reduction}$, and $f_{reduced}$ values varied among collections (Figure 4), but they showed no clear relationships (not shown) with the corresponding precipitation amounts and temperatures (Figure S1). The total $F_{reduction}$ values of the 12 collections accounted for 1.0 ± 0.2% (0.7–1.3%) of the bulk N of the mosses (21 ± 2 mg-N/g, dw; Dong et al., 2017). The $F_{reduction}$ values increased linearly with increasing F_{influx} (Figure 5a). Higher $f_{reduced}$ values occurred for higher F_{influx} and $F_{reduction}$ values (Figure 5b), and in particular, both higher F_{influx} and $F_{reduction}$ occurred for $\Phi_{soil}/\Phi_{atm} > 1.0$ (Figure 5c).

4. Discussion

4.1. Moss NO_3^- Availability

Unlike the leaf NO_3^- of vascular plants, which is mainly influenced by soil NO_3^- availability (Jones et al., 2008), the $[NO_3^-]_{pool}$ in mosses has been previously assumed to respond more sensitively to atmospheric NO_3^- levels (Liu, Koba, Liu, et al., 2012; Liu, Koba, Takebayashi, et al., 2012). When comparing the four species from the same collection, the $[NO_3^-]_{pool}$ did differ somewhat (Figure S1), presumably because of differences in the moss NO_3^- acquisition and the NRA associated with the microhabitats. However, when considering all of the collections, no significant differences in $[NO_3^-]_{pool}$ were observed among the investigated moss species (Figures 2aand S3). Moreover, the four different moss species had similar $[NO_3^-]_{pool}$ dynamics over the 13-month sampling period (Figure 2a). These results suggest that moss NO_3^- uptake and accumulation is less a function of species identity, but it is rather more significantly influenced by environmental NO_3^- availability. This finding on moss NO_3^- uptake is consistent with that of tracer studies, which showed that the concentrations of applied $^{15}NO_3^-$ in mosses did not differ significantly between species, but they did differ significantly between doses of $^{15}NO_3^-$ applications or sites with different levels of atmospheric N deposition (Ayres et al., 2006; Wang et al., 2014; Wiedermann et al., 2009). In contrast, Wanek and Pörtl (2008) found that the kinetic constants of $^{15}NO_3^-$ uptake differed significantly between moss species, but not between bryophytes colonizing different microhabitats.

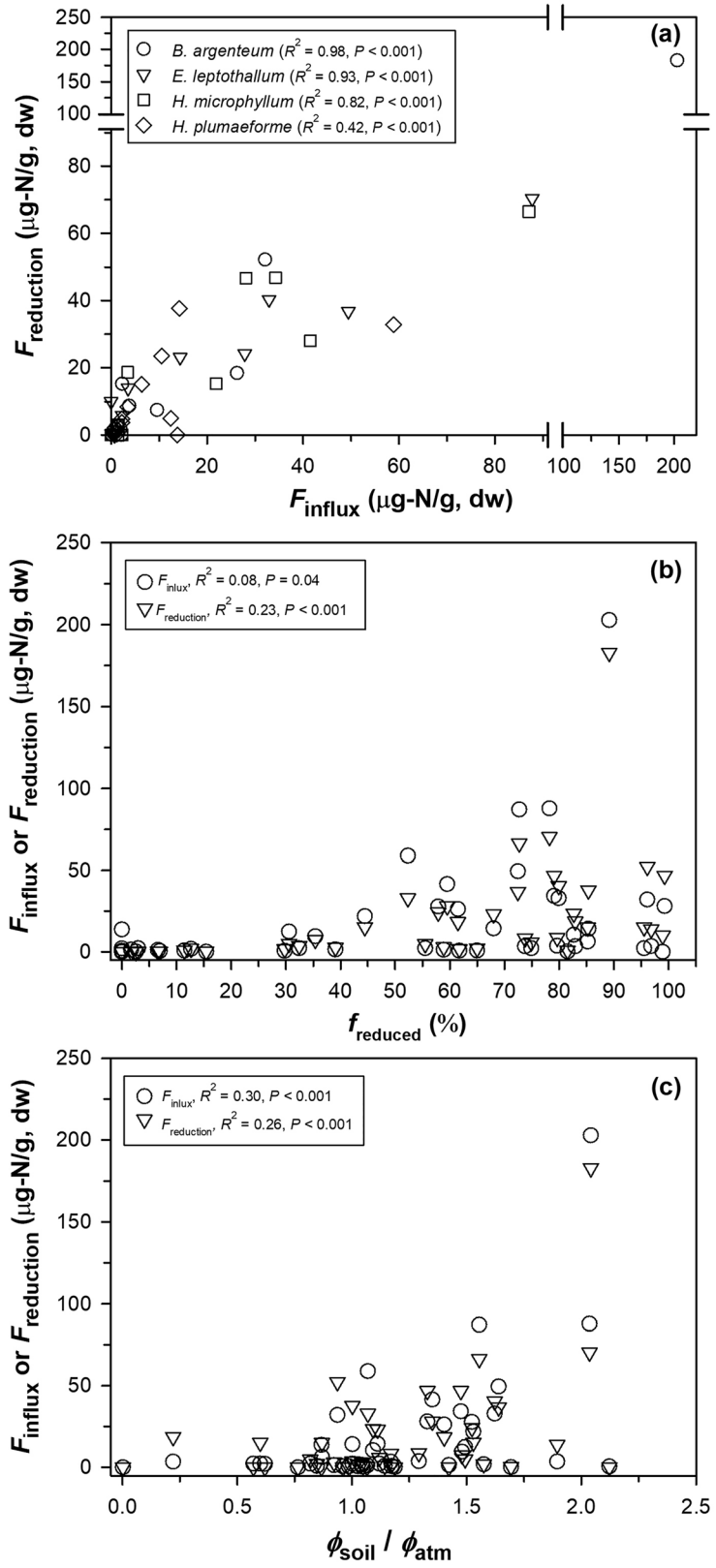

Figure 5. (a) Correlation between F_{influx} and $F_{reduction}$, (b) variations in $f_{reduced}$ with F_{influx} and $F_{reduction}$, and (c) variations in F_{influx} and $F_{reduction}$ with Φ_{soil}/Φ_{atm} (the Φ_{soil}/Φ_{atm} of 21.2 for *Eurohypnum leptothallum* collected on 28 July 2007 was not considered in the correlation) for the epilithic mosses from Mt. Guanfeng in Guiyang, SW China.

The observed lack of species effect is noteworthy, as it indicates that both single and mixed moss species yield comparable results when used for qualitative monitoring of NO_3^- loading in their growth environments. Nevertheless, the substantial monthly variation in our study cautions against the traditional practice in which $[NO_3^-]_{pool}$ analyses conducted at a single time point were used to infer environmental NO_3^- availabilities on seasonal or annual time scales. At our study site, the precipitation NO_3^- concentrations were actually much higher in the cooler months (particularly in winter due to the urban NO_x pollution from coal combustion) than in the warmer months (Liu et al., 2017). In addition, our study site is located in the subtropical zone, with a mean annual temperature of 16.2°C and a relatively warm climate in winter (Figure S1). In December of 2018, Dong et al. (2019) also observed substantially high NO_3^- concentrations and net nitrification rates in soils of epilithic mosses. Thus, high moss F_{influx} and $[NO_3^-]_{pool}$ values are likely to occur in the winter (e.g., December of 2006) compared to the warmer months (e.g., April, May, or June of 2007) (Figures 4b and S2).

4.2. Moss NO_3^- Sources

The moss-tissue NO_3^- had much lower $\delta^{18}O$ values than the precipitation NO_3^- (Figure 3), indicating the distinct contributions of soil-NO_3^- to the NO_3^- in terrestrial mosses even in epilithic habitats. The distribution of the $\delta^{18}O_{moss}$ values between those of atm-NO_3^- and soil-NO_3^- (Figure 3) as well as our previous $\Delta^{17}O_{moss}$ signatures (Liu et al., 2014) does support the mixing of atm-NO_3^- and soil-NO_3^-. Based on the sampling in July 2010 in Guiyang, mosses on different substrates had $\Delta^{17}O_{moss}$ values (0.8–13.0‰; Liu et al., 2014) much lower than those of the NO_3^- of the local precipitation (19.0–25.4‰; Liu et al., 2018), indicating that atm-NO_3^- is not the sole source of moss NO_3^-. At the present study site, the $\Delta^{17}O$ values of the NO_3^- in the epilithic mosses collected in July 2010 (5.3 ± 5.0‰; Liu et al., 2014) were also lower than those of NO_3^- in precipitation (22.4 ± 3.2‰; Liu et al., 2018). These results suggest that contributions of soil-NO_3^- should be considered when evaluating the responses of moss $[NO_3^-]_{pool}$ to atmospheric NO_3^- pollution in city environments (Liu, Koba, Liu, et al., 2012; Liu, Koba, Takebayashi, et al., 2012). Furthermore, the traditional assumption that epilithic mosses derive nutrients (including NO_3^-) solely from the atmosphere should be modified accordingly.

Together, dual ^{15}N and ^{18}O signals of the NO_3^- in epilithic mosses contain information on both source contributions and the degree of enzymatic reduction in plants (Liu et al., 2013, 2014). In this study, the $\delta^{15}N_{moss}$ values were higher than those of both the atm-NO_3^- and soil-NO_3^- sources (Figure 3), demonstrating that the isotopes of the moss-tissue NO_3^- cannot be explained solely by the mixing of atm-NO_3^- and soil-NO_3^-, rather NO_3^- reduction and the accompanying ^{15}N fractionation in the mosses must also be taken into account. Accordingly, the isotopic effects of NO_3^- reduction should be considered when determining the atm-NO_3^- and soil-NO_3^- contributions to the total NO_3^- influx of mosses (equations 14 and 15).

4.3. Contributions of Atm-NO_3^- and Soil-NO_3^- to Moss-Tissue NO_3^-

In this study, the average Φ_{soil} values based on natural isotopes (equations 1 and 15) were 53 ± 13% (Figures 4a and 4b). Previously, the average fraction of soil-derived N was determined to be 10% in a short-term study (7 days) of mat-forming mosses using labeled ^{15}N-NO_3^-:^{15}N-NH_4^+ (1:1) additions (Ayres et al., 2006), and the mean fractions of ^{15}N tracer recovery in the mosses from the ^{15}N-NO_3^- spiked soils of an alpine meadow were 17–30% (Wang et al., 2014). These fractional contribution values cannot be directly compared due to differences in the methods used. The lower fractional values obtained in short-term tracer studies may be influenced by the rapid movement and partial microbial fixation of the $^{15}NO_3^-$ injected into the soils, resulting in much lower fractions than those of the atmospheric sources. Our new results, based on natural isotopes and multiple samplings, highlight the high uptake of soil NO_3^- by epilithic mosses. The common and high uptake of soil-NO_3^- in terrestrial mosses indicates that moss NO_3^- concentrations and isotopes cannot be used to accurately monitor the degree of atmospheric NO_3^- pollution and to interpret the sources of NO_x emissions (Liu, Koba, Liu, et al., 2012; Liu, Koba, Takebayashi, et al., 2012; Liu et al., 2017). The high soil-NO_3^- availability for epilithic mosses also indicates active microbial nitrification on rock surfaces before and/or after colonization by mosses. The net nitrification rates were determined to be 1.9 ± 0.7 μg-N/g/day and 0.2 ± 0.1 μg-N/g/day in soil substrates of epilithic mosses growing on limestone and sandstone in SW China, respectively (Dong et al., 2019).

Mechanistically, pioneer microbes (bacteria and fungi), algae, and lichens often form a weathering interface between epilithic mosses and the underlying rocks (Raven et al., 1998). Microbial nitrification can proceed in moss soil substrates along with inputs of N from dead microbes, decomposing moss tissues, dry particulate deposition, and wet N deposition (Dong et al., 2019). Diffusion or movement of soil-NO_3^- into moss tissues can occur due to the high mobility of NO_3^- and the fact that the mosses can efficiently absorb and retain water from precipitation, which can extend the interactions between the mosses, water, and substrates. In addition to N acquisition through moss tissues attached on soil substrates, mosses can also translocate soil-NO_3^- from basal tissues up to growing tissues. Tracer studies have revealed that active $^{15}NO_3^-$ translocation from basal moss tissues to upper apical tissues is an important process in moss N budgets (Eckstein & Karlsson, 1999; Gerdol, 1990; Skre et al., 1983), which also supports the high uptake of soil-NO_3^-. For *Sphagnum* mosses, inorganic N translocation contributed 0.5–11% of the annual N requirements, and the N translocation increased under high N deposition (Aldous, 2002).

4.4. Moss NO_3^- Reduction

The reduction of NO_3^- by the enzyme of NR includes two important mechanisms that have rarely been verified in field studies of terrestrial plants, that is, the induction of NRA by NO_3^- supply/uptake (influx) and the inhibition or down regulation of NRA by the assimilation of reduced N forms (Kronzucker et al., 1999; Li et al., 2013; Tischner, 2000). According to Tcherkez and Hodges (2008), if the NO_3^- availability and uptake are low such that the NO_3^- influx becomes limiting compared to the potential reduction rates, then the tissue NO_3^- accumulation will be low. Conversely, if the external NO_3^- availability and plant NO_3^- influx are high, relatively higher amounts of NO_3^- will accumulate. However, few studies have examined how plant NO_3^- accumulation and reduction change with NO_3^- influx under field conditions. In this study, to examine the relationships among F_{influx}, $F_{reduction}$, and $f_{reduced}$ allows us to explore mechanisms of moss NRA discussed above.

The presence of NO_3^- is not obligatory for NR formation, but the rate of NR synthesis and NRA can be stimulated by the NO_3^- supply (Tischner, 2000). Previously, NO_3^- reduction has often been expressed as the rate of the initial NO_3^- consumption or the new NO_2^- production via isotopic labeling (e.g., ^{15}N and ^{13}N; Kronzucker et al., 1999; Simon & Rennenberg, 2014) or traditional in vitro NRA assays (Koba et al., 2003; Koyama et al., 2001). However, these methods cannot assess the in situ reduction of NO_3^- in plants. For mosses, increased NRA has been observed in artificial soil and airborne N supplies (Norby et al., 1989; Woodin et al., 1985; Woodin & Lee, 1987). However, it has not been determined whether moss NO_3^- reduction under field conditions increases with NO_3^- influx and which NO_3^- supply, that is, atm-NO_3^- or soil-NO_3^-, has a greater influence on the NO_3^- reduction in terrestrial mosses. Until now, the approximation of the mean $\delta^{15}N$ values of the NO_3^- in mosses at a single time point (−1.7‰) and the NO_3^- in precipitation (−1.9‰) (Liu, Koba, Takebayashi, et al., 2012) were assumed to reflect the overall inhibition of NO_3^- reduction by the high deposition rate of reduced N in Guiyang (Liu, Koba, Takebayashi, et al., 2012). In this study, the monthly $f_{reduced}$ values ranged between 0% and 99% (Figure 4d), with an average of 50 ± 35% for all 48 collections. This provides natural isotopic evidence for the occurrence of moss NO_3^- reduction and the lack of substantial inhibition of NO_3^- reduction due to the high deposition of reduced N at our study site.

The monthly $f_{reduced}$ and $F_{reduction}$ values varied significantly among collections and species (Figures 4c and 4d), which is not only associated with the different NR regulatory properties from one moss sample to another but also with the strength of the external NO_3^- influx. The monthly $F_{reduction}$ values increased linearly with increasing monthly F_{influx} although the slope differed among the moss species (Figure 5a). In addition, the $f_{reduced}$ values were higher under higher F_{influx} values (Figure 5b). These results suggest that the NO_3^- reduction in mosses is induced by the NO_3^- influx. This is consistent with the previous conclusion that higher NO_3^- availability and influx cause higher NRA and ^{15}N discriminations and vice versa (Liu, Koba, Yoh, & Liu, 2012; Liu, Koba, Takebayashi, et al., 2013; Bloom et al., 2014). Interestingly, the $F_{reduction}$ values increase with increasing F_{influx} (Figure 5a) and both F_{influx} and $F_{reduction}$ became higher when the Φ_{soil}/Φ_{atm} values were higher than 1.0 (Figure 5c). In principal, the source type of plant NO_3^- cannot regulate tissue NO_3^- concentrations and influence

plant NO_3^- reduction, but the availability or supply strength of a specific source NO_3^- can. However, our results suggest that the NO_3^- supply from the soil substrates had a greater influence on the NO_3^- uptake and reduction in epilithic mosses than atm-NO_3^-. This may be related to the steadier availability of soil-NO_3^- to the mosses relative to the intermittent supply of atm-NO_3^- to the mosses, mainly in the form of wet deposition.

4.5. Contributions of NO_3^- Assimilation to the Bulk N of the Mosses

The incorporation of NO_3^- into plant biomass requires more energy than the incorporation of reduced N forms (Li et al., 2013). From the energetic consideration, both moss NO_3^- uptake and reduction have been found to be inhibited by a high N supply, especially when the supply of reduced N forms was higher than that of NO_3^- (Liu, Koba, Makabe, & Liu, 2013; Liu, Koba, Takebayashi, et al., 2012). Several studies have stressed that moss species prefer reduced N forms over NO_3^- and that NRA is inhibited by coexisting NH_4^+-N and/or amino acids (Press & Lee, 1982; Soares & Pearson, 1997; Wanek & Pörtl, 2008; Wiedermann et al., 2009; Woodin et al., 1985; Woodin & Lee, 1987). High N deposition (>10 kg-N/ha/yr) and ambient NO_x also suppress moss NRA (Gordon et al., 2001; Morgan et al., 1992). At our study site, the mosses strongly preferred to assimilate NH_4^+ under high deposition of reduced N (Liu, Koba, Takebayashi, et al., 2013; Dong et al., 2017). Our results reveal that the NRA was incompletely inhibited by reduced N forms, and thus, the contributions of NO_3^- assimilation to the bulk N of the mosses should be reevaluated (Liu, Koba, Liu, et al., 2012; Liu, Koba, Takebayashi, et al., 2012; Liu, Koba, Makabe, & Liu, 2013). Among the 48 collections of four species, six of the collections had $F_{reduction}$ values of 0.0 μg-N/g (i.e., no occurrence of reduction), but this is more likely attributed to the corresponding low F_{influx} values (Figure 5a), not to the inhibition of NR by reduced N assimilation. On average, the four moss species had a total annual $F_{reduction}$ of 219.7 ± 30.5 μg-N/g, dw, which accounted for only 1.0 ± 0.2% of the bulk N of the mosses (21 ± 2 mg/g; Dong et al., 2017).

These results not only provide quantitative evidence for the substantial occurrence of NO_3^- reduction and the probable lack of substantial inhibition of NRA in mosses but also allow us to assess the contribution of NO_3^- assimilation to bulk N assimilation by mosses. At our study site, low contributions of NO_3^- assimilation to the bulk N of epilithic mosses supports our previous interpretations of the bulk $\delta^{15}N$ signatures of mosses based on the dominant assimilation of ammonium and dissolved organic N sources (Dong et al., 2017; Liu, Koba, Takebayashi, et al., 2013). Among the studied moss species, the acrocarpous moss *B. argenteum* is a nitrophilous species (Schwarz & Frahm, 2013). Although variance components show a generally lower contribution of the species than other factors to the variations in the measured and calculated parameters (Figure S3), the distinctly higher $F_{reduction}$ values of *B. argenteum* and the lower $F_{reduction}$ values of *H. plumaeforme* compared to the other two moss species reflect interspecies differences in NO_3^- uptake and reduction. This information can help us understand the response and adaption of moss species distributions under different NO_3^- pollution conditions.

5. Conclusions

Given that the supply and availability of NO_3^- to terrestrial plants is constantly changing due to anthropogenic N emissions, it is necessary to explore how plants' NO_3^- metabolisms will respond to environmental N loading. In this study, we used dual N and O isotopic analyses to determine that the soil NO_3^- contributed about half of the moss-tissue NO_3^- and that substantial reduction of NO_3^- occurs in epilithic mosses. The isotopic evidence presented in our study suggests that atmospheric deposition is not the sole source of NO_3^- for terrestrial mosses as conventionally thought and highlights the fact that soil-NO_3^- influences the pool size and reduction of NO_3^- in terrestrial mosses. As such, future studies should consider the effects of N uptake from soil substrates on ecophysiological processes and functions in mosses when evaluating moss N economy and the influence of atmospheric N pollution on mosses. This study also provides a useful modeling approach for the quantitative evaluation of moss NO_3^- availability and in situ NO_3^- reduction in terrestrial plants. Our results improve our knowledge of cellular NO_3^- behaviors in moss bio-indicators and exemplify the power of isotopic techniques in improving our understanding of the biogeochemistry of atmospheric N pollutants in plant tissues.

Acknowledgments

This study was supported by the State Key Project of Research and Development Plan (2016YFA0600802), the National Natural Science Foundation of China (41730855, 41522301, 41273026), the Kyoto University Foundation, the Sumitomo Foundation together with NEXT Program (GS008) and KAKENHI (26252020 and 26550004) from Japan Society for Promotion of Science (JSPS), a grant-in-aid for scientific research from JSPS (P09316), the 11st Recruitment Program of Global Experts (the Thousand Talents Plan) for Young Professionals granted by the central budget of China. We sincerely thank Dr. Guillaume Tcherkez for constructive comments on the data interpretation of this paper. Thanks to Dr. Robert M. Ellam (an honorary professor in ISESS of Tianjin University) for language corrections. Data of this manuscript have been deposited online (https://datadryad.org/stash/dataset/doi:10.5061/dryad.gxd2547g6).

References

Aerts, R. (1996). Nutrient resorption from senescing leaves of perennials: Are there general patterns? *Journal of Ecology*, *84*, 597–608. https://doi.org/10.2307/2261481

Aldous, A. R. (2002). Nitrogen translocation in *Sphagnum* mosses: Effects of atmospheric nitrogen deposition. *New Phytologist*, *156*, 241–253. https://doi.org/10.1046/j.1469-8137.2002.00518.x

Atkin, O. K., & Cummins, W. R. (1994). The effect of root temperature on the induction of nitrate reductase activities and nitrogen uptake rates in arctic plant species. *Plant & Soil*, *159*(2), 187–197. https://doi.org/10.1007/bf00009280

Atkin, O. K., Villar, R., & Cummins, W. R. (1993). The ability of several high arctic plant species to utilize nitrate-nitrogen under field conditions. *Oecologia*, *96*(2), 239–245. https://doi.org/10.1007/BF00317737

Ayres, E., Van der Wal, R., Sommerkorn, M., & Bardgett, R. D. (2006). Direct uptake of soil nitrogen by mosses. *Biology Letters*, *2*, 286–288. https://doi.org/10.1098/rsbl.2006.0455

Beevers, L., & Hageman, R. H. (1980). Nitrate and nitrite reduction. In B. J. Miflin (Ed.), *The biochemistry of plants*, (Vol. 5, pp. 115–168). New York: Academic Press. https://doi.org/10.1016/B978-0-12-675405-6.50009-7

Bloom, A. J., Burger, M., Kimball, B. A., & Pinter, Jr. P. J. (2014). Nitrate assimilation is inhibited by elevated CO_2 in field-grown wheat. *Nature Climate Change*, *4*, 477–480. https://doi.org/10.1038/nclimate2183

Bloom, A. J., Sukrapanna, S. S., & Warner, R. L. (1992). Root respiration associated with ammonium and nitrate absorption and assimilation by barley. *Plant Physiology*, *99*(4), 1294–1301. https://doi.org/10.1104/pp.99.4.1294

Bragazza, L., Limpens, J., Gerdol, R., Grosvernier, P., Hájek, M., Hájek, T., et al. (2005). Nitrogen concentration and $\delta^{15}N$ signature of ombrotrophic *Sphagnum* mosses at different N deposition levels in Europe. *Global Change Biology*, *11*, 106–114. https://doi.org/10.1111/j.1365-2486.2004.00886.x

Casciotti, K. L., Sigman, D. M., Hasting, G. M., Böhlke, J. K., & Hilkert, A. (2002). Measurement of the oxygen isotopic composition of nitrate in seawater and freshwater using the denitrifier method. *Analytical Chemistry*, *74*, 4905–4912. https://doi.org/10.1021/ac020113w

Craine, J. M., Brookshire, E. N. J., Cramer, M. D., Hasselquist, N. J., Koba, K., Marin-Spiotta, E., & Wang, L. (2015). Ecological interpretations of nitrogen isotope ratios of terrestrial plants and soils. *Plant & Soil*, *396*(1-2), 1–26. https://doi.org/10.1007/s11104-015-2542-1

Dong, Y. P., Huang, H., Song, W., Sun, X. C., Wang, M., Zhang, W., et al. (2019). Natural ^{13}C and ^{15}N dynamics of moss-substrate systems on limestones and sandstones in a karst area of subtropical China. *Catena*, *180*, 8–15. https://doi.org/10.1016/j.catena.2019.04.015

Dong, Y. P., Liu, X. Y., Sun, X. C., Song, W., Zheng, X. D., Li, R., & Liu, C. Q. (2017). Inter-species and intra-annual variations of moss nitrogen utilization: Implications for nitrogen deposition assessment. *Environmental Pollution*, *230*, 506–515. https://doi.org/10.1016/j.envpol.2017.06.058

Eckstein, R. L., & Karlsson, P. S. (1999). Recycling of nitrogen among segments of *Hylocomium splendens* as compared with *Polytrichum commune*: Implications for clonal integration in an ectohydric bryophyte. *Oikos*, *86*, 87–96. https://doi.org/10.2307/3546572

Evans, R. D., Bloom, A. J., Sukrapanna, S. S., & Ehleringer, J. R. (1996). Nitrogen isotope composition of tomato (*Lycopersicon esculentum* Mill. Cv. T-5) grown under ammonium or nitrate nutrition. *Plant Cell & Environment*, *19*, 1317–1323. https://doi.org/10.1111/j.1365-3040.1996.tb00010.x

Galloway, J. N., Townsend, A. R., Erisman, J. W., Bekunda, M., Cai, Z., Freney, J. R., et al. (2008). Transformation of the nitrogen cycle: Recent trends, questions, and potential solutions. *Science*, *320*, 889–892. https://doi.org/10.1126/science.1136674

Gerdol, R. (1990). Vegetation patterns and nutrient status of two mixed mires in the southern Alps. *Journal of Vegetation Science*, *1*, 663–668. https://doi.org/10.2307/3235573

Glime, J.M. (2007). Bryophyte Ecology, Volume 1. *Physiological ecology*. E-book sponsored by Michigan Technological University and the International Association of Bryologists. http://digitalcommons.mtu.edu/bryophyte-ecology

Gordon, C., Wynn, J. M., & Woodin, S. J. (2001). Impacts of increased nitrogen supply on high Arctic heath: The importance of bryophytes and phosphorus availability. *New Phytologist*, *149*, 461–471. https://doi.org/10.1046/j.1469-8137.2001.00053.x

Granger, J., Sigman, D. M., Needoba, J. A., & Harrison, P. J. (2004). Coupled nitrogen and oxygen isotope fractionation of nitrate during assimilation by cultures of marine phytoplankton. *Limnology and Oceanography*, *49*, 1763–1773. https://doi.org/10.4319/lo.2004.49.5.1763

Granger, J., Sigman, D. M., Rohde, M. M., Maldonado, M. T., & Tortell, P. D. (2010). N and O isotope effects during nitrate assimilation by unicellular prokaryotic and eukarotic plankton cultures. *Geochimica et Cosmochimica Acta*, *74*, 1030–1040. https://doi.org/10.1016/j.gca.2009.10.044

Hobbie, E. A., & Högberg, P. (2012). Nitrogen isotopes link mycorrhizal fungi and plants to nitrogen dynamics. *New Phytologist*, *196*, 367–382. https://doi.org/10.1111/j.1469-8137.2012.04300.x

Jones, M. E., Paine, T. D., & Fenn, M. E. (2008). The effect of nitrogen additions on oak foliage and herbivore communities at sites with high and low atmospheric pollution. *Environmental Pollution*, *151*, 434–442. https://doi.org/10.1016/j.envpol.2007.04.020

Jónsdóttir, I. S., Callaghan, T. V., & Lee, J. A. (1995). Fate of added nitrogen in a moss-sedge Arctic community and effects of increased nitrogen deposition. *Science of the Total Environment*, *160*, 677–685. https://doi.org/10.1016/0048-9697(95)04402-M

Kaneko, M., & Poulson, S. R. (2013). The rate of oxygen isotope exchange between nitrate and water. *Geochimica et Cosmochimica Acta*, *118*, 148–156. https://doi.org/10.1016/j.gca.2013.05.010

Kendall, C., Elliott, E. M., & Wankel, S. D. (2007). Tracing anthropogenic inputs of nitrogen to ecosystems. In R. M. Michener, & K. Lajtha (Eds.), *Stable isotopes in ecology and environmental science* (2nd ed., chapter 12, pp. 375–449). Blackwell, Oxford Press. https://doi.org/10.1002/9780470691854.ch12

Koba, K., Hirobe, M., Koyama, L., Kohzu, A., Tokuchi, N., Nadelhoffer, K., et al. (2003). Natural ^{15}N abundance of plants and soil N in a temperate coniferous forest. *Ecosystems*, *6*, 457–469. https://doi.org/10.1007/s10021-002-0132-6

Koyama, L., Tokuchi, N., Hirobe, M., & Koba, K. (2001). The potential of NO_3^--N utilization by a woody shrub species *Lindera triloba*: A cultivation test to estimate the saturation point of soil NO_3^--N for plants. *The Scientific World*, *1*, 514–517. https://doi.org/10.1100/tsw.2001.378

Kronzucker, H. J., Glass, A. D. M., & Siddiqi, M. Y. (1999). Inhibition of nitrate uptake by ammonium in Barley. Analysis of component fluxes. *Plant Physiology*, *120*, 283–291. https://doi.org/10.1104/pp.120.1.283

Ledgard, S. F., Woo, K. C., & Bergersen, F. J. (1985). Isotopic fractionation during reduction of nitrate and nitrite by extracts of spinach leaves. *Functional Plant Biology*, *12*, 631–640. https://doi.org/10.1071/PP9850631

Li, S. X., Wang, Z. H., & Stewart, B. A. (2013). Responses of crop plants to ammonium and nitrate N. In D. L. Sparks (Ed.), *Advances in agronomy* (pp. 205–398). Waltham, MA, USA: Elsevier Academic Press. https://doi.org/10.1016/B978-0-12-405942-9.00005-0

Liu, X. Y., Koba, K., Koyama, L., Hobbie, S. E., Weiss, M. S., Inagaki, Y., et al. (2018). Nitrate is an important nitrogen source for arctic tundra plants. *Proceedings of the National Academy of Sciences of the United States of America*, *115*, 3398–3403. https://doi.org/10.1073/pnas.1715382115

Liu, X. Y., Koba, K., Liu, C. Q., Li, X. D., & Yoh, M. (2012). Pitfalls and new mechanisms in moss isotope biomonitoring of atmospheric nitrogen deposition. *Environmental Science & Technology*, *46*, 12,557–12,566. https://doi.org/10.1021/es300779h

Liu, X. Y., Koba, K., Makabe, A., & Liu, C. Q. (2013). Ammonium first: Natural mosses prefer atmospheric ammonium but vary utilization of dissolved organic nitrogen depending on habitat and nitrogen deposition. *New Phytologist*, *199*(2), 407–419. https://doi.org/10.1111/nph.12284

Liu, X. Y., Koba, K., Makabe, A., & Liu, C. Q. (2014). Nitrate dynamics in natural plants: Insights based on the concentration and natural isotope abundances of tissue nitrate. *Frontiers in Plant Science*, *5*, 1–14. https://doi.org/10.3389/fpls.2014.00355

Liu, X. Y., Koba, K., Takebayashi, Y., Liu, C. Q., Fang, Y. T., & Yoh, M. (2012). Preliminary insights into $\delta^{15}N$ and $\delta^{18}O$ of nitrate in natural mosses: A new application of the denitrifier method. *Environmental Pollution*, *162*, 48–55. https://doi.org/10.1016/j.envpol.2011.09.029

Liu, X. Y., Koba, K., Takebayashi, Y., Liu, C. Q., Fang, Y. T., & Yoh, M. (2013). Dual N and O isotopes of nitrate in natural plants: First insights into individual variability and organ-specific patterns. *Biogeochemistry*, *114*(1-3), 399–411. https://doi.org/10.1007/s10533-012-9721-4

Liu, X. Y., Koba, K., Yoh, M., & Liu, C. Q. (2012). Nitrogen and oxygen isotope effects of tissue nitrate associated with nitrate acquisition and utilization in the moss *Hypnum plumaeforme*. *Functional Plant Biology*, *39*, 598–608. https://doi.org/10.1071/FP12014

Liu, X. Y., Xiao, H. W., Xiao, H. Y., Song, W., Sun, X. C., & Liu, C. Q. (2017). Stable isotope analyses of precipitation nitrogen sources in Guiyang, southwestern China. *Environmental Pollution*, *230*, 486–494. https://doi.org/10.1016/j.envpol.2017.06.010

Liu, X. Y., Xiao, H. Y., Liu, C. Q., & Li, Y. Y. (2007). $\delta^{13}C$ and $\delta^{15}N$ of moss *Haplocladium microphyllum* (Hedw.) Broth. for indicating growing environment variation and canopy retention on atmospheric nitrogen deposition. *Atmospheric Environment*, *41*, 4897–4907. https://doi.org/10.1016/j.atmosenv.2007.02.004

Mariotti, A., Mariotti, F., Champigny, M. L., Amarger, N., & Moyse, A. (1982). Nitrogen isotope fractionation associated with nitrate reductase activity and uptake of NO_3^- by pearl millet. *Plant Physiology*, *69*(4), 880–884. https://doi.org/10.1104/pp.69.4.880

Michalski, G., Meixner, T., Fenn, M., Hernandez, L., Sirulnik, A., Allen, E., & Thiemens, M. (2004). Tracing atmospheric nitrate deposition in a complex semiarid ecosystem using $\Delta^{17}O$. *Environmental Science & Technology*, *38*, 2175–2181. https://doi.org/10.1021/es034980+

Morgan, S. M., Lee, J. A., & Ashenden, T. W. (1992). Effects of nitrogen oxides on nitrate assimilation in bryophytes. *New Phytologist*, *120*, 89–97. https://doi.org/10.1111/j.1469-8137.1992.tb01061.x

Nadelhoffer, K. J., Shaver, G., Fry, B., Giblin, A., Johnson, L., & McKane, R. (1996). ^{15}N natural abundances and N use by tundra plants. *Oecologia*, *107*(3), 386–394. https://doi.org/10.1007/BF00328456

Norby, R. J., Weerasuriya, Y., & Hanson, P. J. (1989). Induction of nitrate reductase activity in red spruce needles by NO_2 and HNO_3 vapor. *Canadian Journal of Forest Research*, *19*, 889–896. https://doi.org/10.1139/x89-135

Paulissen, M. P. C. P., van der Ven, P. J. M., Dees, A. J., & Bobbink, R. (2004). Differential effects of nitrate and ammonium on three fen bryophyte species in relation to pollution nitrogen input. *New Phytologist*, *164*, 451–458. https://doi.org/10.1111/j.1469-8137.2004.01196.x

Press, M. C., & Lee, J. A. (1982). Nitrate reductase activity of *Sphagnum* species in the South Pennines. *New Phytologist*, *92*, 487–494. https://doi.org/10.1111/j.1469-8137.1982.tb03406.x

Raven, J. A., Griffiths, H., Smith, E. C., & Vaughn, K. C. (1998). New perspectives in the biophysics and physiology of bryophytes. In J. W. Bates, N. W. Ashton, & J. G. Duckett (Eds.), *Bryology in the twenty-first century* (pp. 261–275). London, UK: Maney Publishing and the British Bryological Society.

Reinhart, D. A., & Thomas, R. J. (1981). Sucrose uptake and transport in conducting cells of *Polytrichum commune*. *Bryologist*, *84*, 59–64. https://doi.org/10.2307/3242978

Robinson, D., Handley, L. L., & Scrimgeour, C. M. (1998). A theory for $^{15}N/^{14}N$ fractionation in nitrate-grown vascular plants. *Planta*, *205*, 397–406. https://doi.org/10.1007/s004250050336

Schwarz, U., & Frahm, J. P. (2013). A contribution to the bryoflora of the Western Ghats in Karnataka state, India. *Polish Botanical Journal*, *58*, 511–524. https://doi.org/10.2478/pbj-2013-0039

Simon, J., Li, X. Y., & Rennenberg, H. (2014). Competition for nitrogen between European beech and sycamore maple shifts in favour of beech with decreasing light availability. *Tree Physiology*, *34*, 49–60. https://doi.org/10.1093/treephys/tpt112

Skre, O., Oechel, W. C., & Miller, P. M. (1983). Patterns of translocation of carbon in four common moss species in a black spruce (*Picea mariana*) dominated forest in interior Alaska. *Canadian Journal of Forest Research*, *13*, 869–878. https://doi.org/10.1139/x83-117

Soares, A., & Pearson, J. (1997). Short-term physiological response of mosses to atmospheric ammonium and nitrate. *Water Air & Soil Pollution*, *93*, 225–242. https://doi.org/10.1023/A:1022110900365

Stewart, G. R., Pate, G. S., & Unkovich, M. (1993). Characteristics of inorganic nitrogen assimilation of plants in fire-prone Mediterranean-type vegetation. *Plant Cell & Environment*, *16*, 351–363. https://doi.org/10.1111/j.1365-3040.1993.tb00881.x

Tcherkez, G., & Farquhar, G. D. (2006). Isotopic fractionation by plant nitrate reductase, twenty years later. *Functional Plant Biology*, *33*, 531–537. https://doi.org/10.1071/FP05284

Tcherkez, G., & Hodges, M. (2008). How stable isotopes may help to elucidate primary nitrogen metabolism and its interactions with (photo)respiration in C_3 leaves. *Journal of Experimental Botany*, *59*, 1685–1693. https://doi.org/10.1093/jxb/erm115

Tischner, R. (2000). Nitrate uptake and reduction in higher and lower plants. *Plant, Cell & Environment*, *23*, 1005–1024. https://doi.org/10.1046/j.1365-3040.2000.00595.x

Wanek, W., & Pörtl, K. (2008). Short-term ^{15}N uptake kinetics and nitrogen nutrition of bryophytes in a lowland rainforest, Costa Rica. *Functional Plant Biology*, *35*, 51–62. https://doi.org/10.1071/FP07191

Wang, J. N., Shi, F. S., Xu, B., Wang, Q., Wu, Y., & Wu, N. (2014). Uptake and recovery of soil nitrogen by bryophytes and vascular plants in an alpine meadow. *Journal of Mountain Science*, *11*(2), 475–484. https://doi.org/10.1007/s11629-013-2707-4

Wania, R., Hietz, P., & Wanek, W. (2002). Natural ^{15}N abundance of epiphytes depends on the position within the forest canopy: Source signals and isotope fractionation. *Plant, Cell & Environment*, *25*, 581–589. https://doi.org/10.1046/j.1365-3040.2002.00836.x

Wells, J. M., & Brown, D. H. (1996). Mineral nutrient recycling within shoots of the moss *Rhytidiadelphus squarrosus* in relation to growth. *Journal of Bryology*, *19*, 1–17. https://doi.org/10.1179/jbr.1996.19.1.1

Werner, R. A., & Schmidt, H. L. (2002). The *in vivo* nitrogen isotope discrimination among organic plant compounds. *Phytochemistry*, *61*, 465–484. https://doi.org/10.1016/S0031-9422(02)00204-2

Wiedermann, M. M., Gunnarsson, U., Ericson, L., & Nordin, A. (2009). Ecophysiological adjustment of two *Sphagnum* species in response to anthropogenic N deposition. *New Phytologist*, *181*(1), 208–217. https://doi.org/10.1111/j.1469-8137.2008.02628.x

Woodin, S. J., & Lee, J. A. (1987). The effects of nitrate, ammonium and temperature on nitrate reductase activity in *Sphagnum* species. *New Phytologist*, *105*, 103–115. https://doi.org/10.1111/j.1469-8137.1987.tb00114.x

Woodin, S. J., Press, M. C., & Lee, J. A. (1985). Nitrate reductase activity in *Sphagnum fuscum* in relation to wet deposition of nitrate from the atmosphere. *New Phytologist*, *99*, 381–388. https://doi.org/10.1111/j.1469-8137.1985.tb03666.x

Yoneyama, T., & Tanaka, F. (1999). Natural abundance of ^{15}N in nitrate, ureides, and amino acids from plant tissues. *Soil Science & Plant Nutrition*, *45*, 751–755. https://doi.org/10.1080/00380768.1999.10415840

Zechmeister, H. G., Richter, A., Smidt, S., Hohenwallner, D., Roder, I., Maringer, S., & Wanek, W. (2008). Total nitrogen content and $\delta^{15}N$ signatures in moss tissue: Indicative value for nitrogen deposition patterns and source allocation on a nationwide scale. *Environmental Science & Technology*, *42*(23), 8661–8667. https://doi.org/10.1021/es801865d